Langmuir



Letter

# Anatase TiO Nanoparticles on Rutile TiO Nanorods: A Heterogeneous Nanostructure via Layer-by-Layer Assembly

Zhaoyue Liu, Xintong Zhang, Shunsuke Nishimoto, Ming Jin, Donald A. Tryk, Taketoshi Murakami, and Akira Fujishima

*Langmuir*, **2007**, 23 (22), 10916-10919 • DOI: 10.1021/la7018023



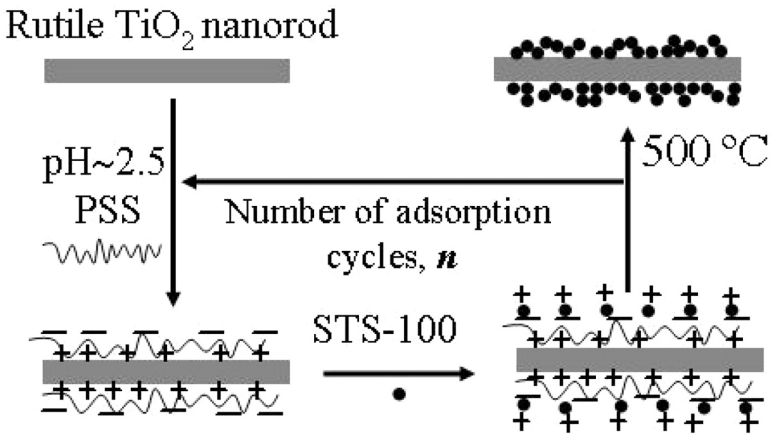


## More About This Article

Additional resources and features associated with this article are available within the HTML version:

- Supporting Information
- Access to high resolution figures
- Links to articles and content related to this article
- Copyright permission to reproduce figures and/or text from this article

View the Full Text HTML

# Anatase $TiO_2$ Nanoparticles on Rutile $TiO_2$ Nanorods: A Heterogeneous Nanostructure via Layer-by-Layer Assembly

Zhaoyue Liu, Xintong Zhang, Shunsuke Nishimoto, Ming Jin, Donald A. Tryk, Taketoshi Murakami, and Akira Fujishima*

*Photocatalyst Group, Special Research Laboratory for Optical Science, Kanagawa Academy of Science and Technology, KSP Building West 614, 3-2-1 Sakado, Takatsu-ku, Kawasaki, Kanagawa 213-0012, Japan*

*Received June 18, 2007. In Final Form: September 6, 2007*

We report here the use of a layer-by-layer assembly technique to prepare novel $TiO_2$ heterogeneous nanostructures in which anatase nanoparticles are assembled on rutile nanorods. The preparation includes assembling anatase nanoparticle multilayers on rutile nanorods via electrostatic deposition using poly(sodium 4-styrene sulfonate) as a bridging or adhesion layer, followed by burning off the polymeric material via calcination. The composition of the heterogeneous nanostructures (i.e., the anatase-to-rutile ratio) can be tuned conveniently by controlling the experimental conditions of the layer-by-layer assembly. It was found that, with the optimum preparation conditions, the heterogeneous nanostructures showed better photocatalytic activity for decomposing gaseous acetaldehyde than either the original anatase nanoparticles or the rutile nanorods. This is discussed on the basis of the synergistic effect of the existence of both rutile and anatase in the heterogeneous nanostructure.

## Introduction

The concept of coupling two different types of semiconductor photocatalytic materials or photoelectrolytic materials in order to enhance electron−hole charge separation and inhibit recombination has been around for quite some time.[1−3] Heterogeneous systems of this type have often involved $TiO_2$ and have attracted a great deal of attention for the development of high-activity photocatalysts.[4−18] For example, anatase/rutile $TiO_2$,[4−8] $TiO_2$/$SnO_2$,[9−12] $TiO_2$/$WO_3$,[13] and $TiO_2$/CdS[14−18] have been studied intensively. In particular, the anatase/rutile $TiO_2$ heterogeneous nanostructure is intriguing because it involves only a change in the crystal structure of the same material. In fact, a synergistic effect has been proposed for the high photocatalytic activity of Degussa P25 $TiO_2$, which contains both anatase and rutile.[19] The coupling of anatase and rutile phase $TiO_2$ allows the transfer of electrons excited by ultraviolet light from anatase to rutile $TiO_2$ as a result of the slightly lower conduction band energy of the rutile phase,[4,20] and thus charge recombination can be suppressed.[4−6] It is necessary to note that this effect does not necessarily involve either sensitization or energy transfer (antenna effect)[21] (i.e., electron−hole pairs are produced in both phases).

Therefore, it is of prime importance to develop effective techniques to fabricate such heterogeneous nanostructures. There have been several reports dealing with the preparation of anatase/rutile heterogeneous nanostructures for powder-type photocatalysts.[6,8] For example, Kawahara et al.[6] prepared anatase/rutile coupled particles by a dissolution−reprecipitation method. Ohno et al.[8] prepared an anatase/rutile mixture by physically mixing anatase and rutile $TiO_2$ particles in water or calcining pure anatase $TiO_2$ powders at different temperature. However, these methods cannot isolate the heterogeneous particles from the pure anatase or rutile particles. Moreover, the ability to control the composition of the heterogeneous nanostructures accurately and conveniently should be developed. Here, we report that anatase/rutile nanostructures can be easily prepared by the layer-by-layer (LbL) assembly technique, which was originally formulated by Decher[22] in general and then was used by several groups for the assembly of nanoparticles.[23−30] By this technique, for the first time, we deposited anatase nanoparticles on the surfaces of 1-D rutile $TiO_2$ nanorods. A prominent merit of the LbL preparation

* Corresponding author: E-mail: fujishima@newkast.or.jp. Fax: +81-44-819-2038. Tel: +81-44-819-2020.

(1) Nozik, A. J. *Appl. Phys. Lett.* **1977**, *30*, 567−569.
(2) Spanhel, L.; Weller, H.; Henglein, A. *J. Am. Chem. Soc.* **1987**, *109*, 6632−6635.
(3) Gopidas, K. R.; Bohorquez, M.; Kamat, P. V. *J. Phys. Chem.* **1990**, *94*, 6435−6440.
(4) Kawahara, T.; Konishi, Y.; Tada, H.; Tohge, N.; Nishii, J.; Ito, S. *Angew. Chem., Int. Ed.* **2002**, *114*, 2935−2937.
(5) Jiang, D.; Zhang, S.; Zhao, H. *Environ. Sci. Technol.* **2007**, *41*, 303−308.
(6) Kawahara, T.; Ozawa, T.; Iwasaki, M.; Tada, H.; Ito, S. *J. Colloid Interface Sci.* **2003**, *267*, 377−381.
(7) Ohno, T.; Sarukawa, K.; Matsumura, M. *J. Phys. Chem. B* **2001**, *105*, 2417−2420.
(8) Ohno, T.; Tokieda, K.; Higashida, S.; Matsumura, M. *Appl. Catal. A* **2003**, *244*, 383−391.
(9) Tada, H.; Hattori, A.; Tokihisa, Y.; Imai, K.; Tohge, N.; Ito, S. *J. Phys. Chem. B* **2000**, *104*, 4585−4587.
(10) Vinodgopal, K.; Bedja, I.; Kamat, P. V. *Chem. Mater.* **1996**, *8*, 2180−2187.
(11) Cao, Y.; Zhang, X.; Yang, W.; Du, H.; Bai, Y.; Li, T.; Yao, J. *Chem. Mater.* **2000**, *12*, 3445−3448.
(12) Vinodgopal, K.; Kamat, P. V. *Environ. Sci. Technol.* **1995**, *29*, 841−845.
(13) Pan, J. H.; Lee, W. I. *Chem. Mater.* **2006**, *18*, 847−853.
(14) Linsebigler, A. L.; Lu, G.; Yates, J. T. *Chem. Rev.* **1995**, *95*, 735−758.
(15) Jang, J. S.; Choi, S. H.; Park, H.; Choi, W.; Lee, J. S. *J. Nanosci. Nanotechnol.* **2006**, *6*, 3642−3646.
(16) Yu, J. C.; Wu, L.; Lin, J.; Li, P. S; Li, Q. *Chem. Commun.* **2003**, 1552−1553.
(17) Serpone, N.; Borgarello, E.; Grätzel, M. *J. Chem. Soc., Chem. Commun.* **1984**, 342−344.
(18) Serpone, N.; Maruthamuthu, P.; Pichat, P.; Pelizzetti, E.; Hidaka, H. *J. Photochem. Photobiol., A* **1995**, *85*, 247−255.
(19) Bickley, R. J.; Gonzalez-Carreno, T.; Lees, J. S.; Palmisano, L.; Tilley, R. D. *J. Solid State Chem.* **1991**, *92*, 178−190.
(20) Tang, H.; Prasad, K.; Sanjines, R.; Schmid, P. E.; Levy, F. *J. Appl. Phys.* **1994**, *75*, 2042−2047.
(21) Hurum, D. C.; Agrios, A. G.; Gray, K. A.; Rajh, T.; Thurnauer, M. C. *J. Phys. Chem. B.* **2003**, *107*, 4545−4549.
(22) Decher, G. *Science* **1997**, *277*, 1232−1237.
(23) Kim, T.; Sohn, B. *Appl. Surf. Sci.* **2002**, *201*, 109−114.
(24) Kotov, N. A.; Dekany, I.; Fendler, J. H. *J. Phys. Chem.* **1995**, *99*, 13065−13069.
(25) Liu, Y.; Wang, A.; Claus, R. *J. Phys. Chem. B* **1997**, *101*, 1385−1388.
(26) Wang, D.; Rogach, A. L.; Caruso, F. *Nano Lett.* **2002**, *2*, 857−861.
(27) Crisp, M. T.; Kotov, N. A. *Nano Lett.* **2003**, *3*, 173−177.
(28) Zhang, X. T.; Sato, O.; Taguchi, M.; Einaga, Y.; Murakami, T.; Fujishima, A. *Chem. Mater.* **2005**, *17*, 696−700.
(29) Zhang, X. T.; Fujishima, A.; Jin, M.; Emeline, A. V.; Murakami, T. *J. Phys. Chem. B* **2006**, *110*, 25142−25148.
(30) Schulze, K.; Kirstein, S. *Appl. Surf. Sci.* **2005**, *246*, 415−419.

10.1021/la7018023 CCC: $37.00 
Published on Web 09/25/2007

**Scheme 1. Flow Chart for the Preparation of $TiO_2$ Heterogeneous Nanostructures by the LbL Assembly Technique**

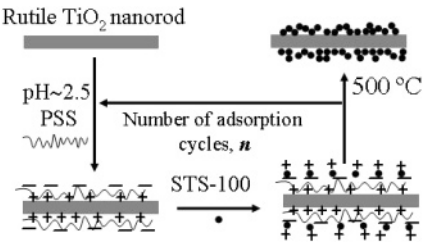


methodology is that it can isolate the heterogeneous nanostructures from the non-adsorbed anatase particles by repeated centrifugation. Furthermore, our experimental conditions are quite mild, and the compositions of the heterogeneous nanostructures can be easily controlled via the parameters of the LbL assembly. It should be mentioned that the use of the long 1-D rutile $TiO_2$ nanorods as described here provides an excellent overall structure in which the resulting anatase/rutile $TiO_2$ heterogeneous nanostructures can be observed distinctly while simultaneously preserving sufficient surface area for the photocatalytic reaction.

## Experimental Section

**Materials.** Rutile $TiO_2$ nanorods (acicular-type $TiO_2$, FTL-200) and an anatase $TiO_2$ colloidal solution (STS-100) were obtained from Ishihara Sangyo Co., Ltd., Japan. Hydrochloric acid (35−37%) and ethanol were obtained from Wako Chemicals. Polyelectrolyte poly(sodium-4-styrenesulfonate) (PSS, 30 wt % solution in water, MW = 70 000) was obtained from Aldrich. Before use, the PSS solution was diluted to 10 g $L^{-1}$ with water. The pH value of the solution was adjusted to about 2.5 with hydrochloric acid. Milli-Q water with a resistivity of 18 MΩ·cm was used in all of the experiments.

**Preparation of the Heterogeneous Nanostructures.** The preparation process of anatase/rutile heterogeneous nanostructures is summarized in Scheme 1. In a typical preparation, 0.2 g of rutile $TiO_2$ nanorods was dispersed in 100 mL of a hydrochloric acid solution (pH ∼2.5) ultrasonically. A 25 mL portion of PSS solution (pH ∼2.5) was added to the $TiO_2$ suspension, and the mixture solution was stirred for 30 min. During this period, PSS was adsorbed on the surface of $TiO_2$ nanorods because the former is negatively charged and the latter is positively charged as a result of the fact that the pH is below the isoelectric point (pH ∼5.9[31]). Thereafter, the nonadsorbed polyelectrolyte was removed by four repeated centrifugation/water wash/redispersion cycles. The polyelectrolyte-coated rutile $TiO_2$ nanorods were redispersed in 100 mL of water, and 2 mL of the anatase $TiO_2$ colloidal solution (STS-100) was added to allow adsorption for 30 min. The nonadsorbed $TiO_2$ particles were also removed by repeated centrifugation. The above adsorption cycles were repeated until the desired number of adsorption cycles, *n*, was reached. Finally, the sample was calcined at 500 °C for 1 h to remove the polymeric material. In the present work, the numbers of cycles used for anatase $TiO_2$ were 3, 5, 7, 9, and 11.

**Characterization.** The diffuse UV−visible absorption spectra of $TiO_2$ powders were recorded on a Shimadzu UV-2450 spectrophotometer equipped with an integrating sphere. Transmission electron microscope (TEM) images were obtained on a Topcon EM-002B high-resolution transmission electron microscope. X-ray diffraction (XRD) patterns were measured on a Rigaku RINT 1500 X-ray diffraction meter using Cu Kα radiation in the range of 20 to 60°. The powders were spread on the surface of a silicon wafer and then used for the XRD measurements.

**Evaluation of the Photocatalytic Activity.** The photocatalytic activity of the heterogeneous nanostructures was evaluated by the gas-phase decomposition of acetaldehyde in a batch-type reactor.[32] The vessel was made from Pyrex glass with a volume of 500 mL. Portions (20 mg) of the photocatalyst powders were spread evenly on the bottom of a glass disk (about 6.2 $cm^2$ area), and this was placed in the reaction vessel. Commercially available pure air (Taiyo Nippon Sanso Corporation) was humidified to about 50% by flowing through a water/ice mixture and introduced into the reaction vessel at room temperature. Then, 8 mL of a reaction gas (1 vol % acetaldehyde in $N_2$, Takachiho, Japan) was introduced into the reaction vessel using a Pressure-Lok syringe. After adsorption in the dark for 1 h, with adsorption equilibrium having been confirmed by the constant concentration of acetaldehyde, the reactor was placed below black-light lamps (Toshiba, FL10BLB, wavelength range of 290−420 nm with a peak at 352 nm), which emit UV light with an irradiance of 1.2 mW/$cm^2$ as measured with a power meter (Hamamatsu Photonics, C9536-01). The decrease in the acetaldehyde concentration was monitored using gas chromatography (GC-8A, Shimadzu, Japan).

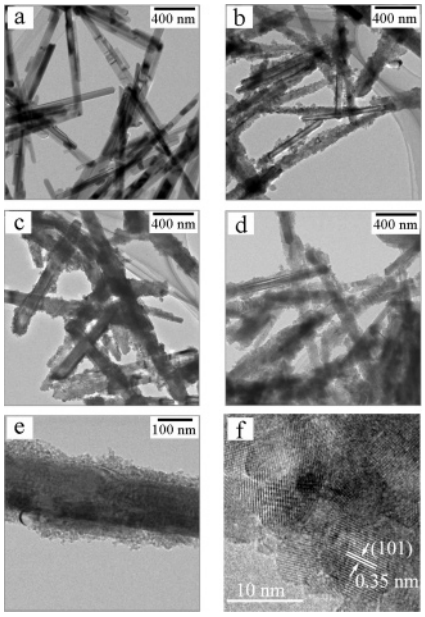


**Figure 1.** TEM images of the original rutile $TiO_2$ nanorods (a) and heterogeneous nanostructures with $n = 5$ (b), 9 (c), and 11 (d). Magnified images of the heterogeneous nanostructure with $n = 11$ (e, f). The heterogeneous nanostructures were all calcined to remove polymer material.

## Results and Discussion

The rutile $TiO_2$ nanorods were found to disperse poorly in water. The addition of PSS solution, however, remarkably improved the state of dispersion. It was thus assumed that the PSS adsorbed on the $TiO_2$ surface, and this resulted in the increase in the surface charge density of the $TiO_2$ nanorods. Even though the sign of the surface charge would then reverse, it is reasonable to propose that the magnitude would increase. The subsequent addition of colloidal anatase solution degraded the dispersibility of the rutile nanorods, indicating the adsorption of small anatase nanoparticles on the larger nanorods by means of the PSS adhesion layer, decreasing the charge density. With the further addition of PSS solution, the suspension again became well-dispersed.

Figure 1a shows a TEM image of the naked rutile $TiO_2$ nanorods. As shown, the diameter is ca. 60−80 nm, and the length is on the order of several micrometers. Alternating treatments with PSS and anatase nanoparticles roughen the smooth

(31) Kosmulski, M. *Adv. Colloid Interface Sci.* **2002**, *99*, 255−264.

(32) Sopyan, I.; Watanabe, M.; Murasawa, S.; Hashimoto, K.; Fujishima, A. *J. Photochem. Photobiol., A* **1996**, *98*, 79−86.

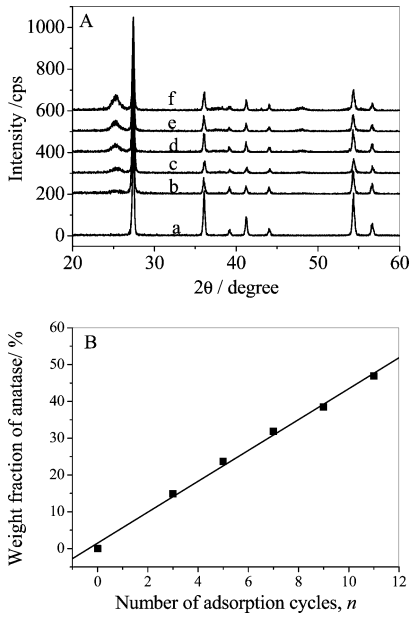


**Figure 2.** (A) XRD patterns of rutile $TiO_2$ nanorods (a) and heterogeneous nanostructures with $n = 3$ (b), 5 (c), 7 (d), 9 (e), and 11 (f). (B) Dependence of the anatase composition in the heterogeneous nanostructures on the number of adsorption cycles of anatase $TiO_2$ particles.

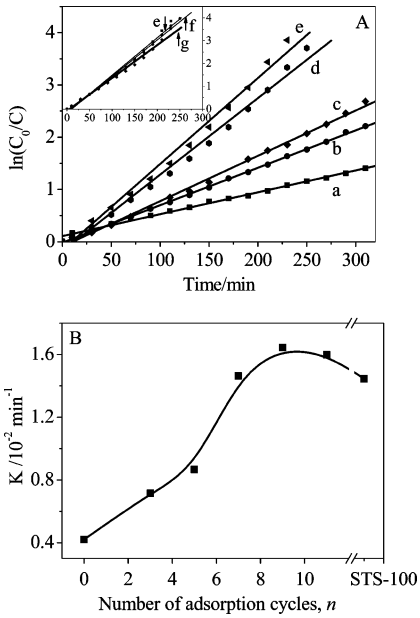


**Figure 3.** (A) Dependence of $\ln(C_0/C)$ on the photocatalytic reaction time $t$ for rutile $TiO_2$ nanorods (a), heterogeneous nanostructures with adsorption cycles $n = 3$ (b), 5 (c), 7 (d), 9 (e), and 11 (f) and the STS-100 sample (g) after calcination for 1 h. (B) Plot of the first-order rate constant for the complete decomposition of acetaldehyde vs the number of adsorption cycles of anatase $TiO_2$.

surface of the nanorods, as shown in Figure 1b−d, clearly indicative of the assembly of the nanoparticles on the nanorods. Magnified images of the heterogeneous nanostructure with $n =$ 11 are shown in Figure 1e,f. As shown, the anatase $TiO_2$ particles (ca. 8 nm diameter) become interconnected to form a porous layer on the nanorod. The high-resolution images show that the anatase particles are fully crystalline, with lattice spacings of 0.35 nm, which corresponds to the (101) crystal plane. Increasing the number of adsorption cycles resulted in the increasing thickness of the anatase layer on the surface of the nanorod. Thus, we were able to control the thickness of the anatase porous layer conveniently by means of the LbL assembly process.

The presence of a crystalline anatase $TiO_2$ component in the heterogeneous nanostructures is further supported by XRD measurements (Figure 2). The naked $TiO_2$ nanorods show the characteristic XRD pattern of the rutile structure (Figure 2A). The strong diffraction peaks at $2\theta = 27.4$, 36.1, 39.2, 41.2, 44.0, 54.4, and 56.7° can be indexed to the (110), (101), (200), (111), (210), (211), and (220) crystal planes of rutile $TiO_2$ (PDF card 75-1755, JCPDS). For the heterogeneous nanostructures, in addition to these peaks, there also exists a peak at $2\theta = 25.3°$ that can be indexed to the (101) plane of anatase $TiO_2$. With the increase in the number of adsorption cycles, the intensity of the latter increased. On the basis of a standard calibration curve (Supporting Information), we calculated that the weight fractions of anatase $TiO_2$ in the heterostructured photocatalysts with $n =$ 3, 5, 7, 9, and 11 were 14.9, 23.7, 31.8, 38.5, and 46.9%, respectively, a nearly linear relation with the number of adsorption cycles (Figure 2B). The weight percentage increment of anatase $TiO_2$ added by every adsorption cycle was rather constant (ca. 4.2%). The uniform weight increase suggests that the deposition of anatase $TiO_2$ nanoparticles on the rutile nanorod proceeded in an orderly fashion, similar to the assembly process on smooth substrates.[23]

The absorption threshold of the heterogeneous nanostructures was determined to be 420 nm from the diffuse UV−visible absorption spectrum (Supporting Information), which was the same as that of the rutile nanorods. In the short-wavelength region, the anatase component caused the absorption of the heterogeneous nanostructures to increase slightly.

We examined the photocatalytic activities of heterogeneous nanostructures, with $n = 3$, 5, 7, 9, and 11 by the decomposition of gaseous acetaldehyde, which is a well-recognized photocatalytic reaction.[32−34] For comparison, the activities of anatase nanoparticles prepared by calcining STS-100 sample at 500 °C for 1 h and rutile nanorods were also measured. These data are shown in Figure 3a. The decomposition of the acetaldehyde on all samples was observed to follow mass transfer-controlled first-order kinetics approximately as a result of the low initial concentration of acetaldehyde (∼150 ppmv),[32−34] as evidenced by the linear plot of $\ln(C_0/C)$ versus photocatalytic reaction time $t$ in minutes. Here, $C_0$ is the initial concentration of acetaldehyde, and $C$ is the concentration of acetaldehyde after photocatalytic reaction for $t$. The first-order kinetic behavior was first observed in a liquid-phase photocatalytic reaction with a low initial concentration of reactant.[35−37] The rate constants of all samples were calculated from Figure 3 a, and these data are plotted in Figure 3B for a clear comparison. It is clearly seen in the two figures that the rate constants for the complete decomposition of acetaldehyde by the heterogeneous nanostructures were greater than that for the original rutile $TiO_2$ nanorods, and the rate constants increased with increasing $n$ from 3 to 9. The rate constant of the heterogeneous nanostructure with $n = 9$ was maximal ($0.017\ min^{-1}$), which exceeded those for the nanostructures with $n = 11$ ($0.016\ min^{-1}$) and for the anatase sample ($0.014\ min^{-1}$).

Considering that anatase generally exhibits better photocatalytic activity for the decomposition of acetaldehyde than rutile,[4,6] it is interesting that the anatase sample did not show higher

(33) Sopyan, I.; Murasawa, S.; Hashimoto, K.; Fujishima, A. *Chem. Lett.* **1994**, 723−726.
(34) Matsubara, H.; Takada, M.; Koyama, S.; Hashimoto, K.; Fujishima, A. *Chem. Lett.* **1995**, 767−768.
(35) Okamoto, K.; Yamamoto, Y.; Tanaka, H.; Tanaka, M.; Itaya, A. *Bull. Chem. Soc. Jpn.* **1985**, *58*, 2015−2022.
(36) Matthews, R. W. *J. Phys. Chem.* **1987**, *91*, 3328−3333.
(37) Al-Ekabi, H.; Serpone, N. *J. Phys. Chem.* **1988**, *92*, 5726−5731.

photocatalytic activity than the heterogeneous nanostructures ($n = 9$) of the same total weight. Note that the latter contained only 38.5% anatase by weight. These results clearly indicate the existence of a synergistic effect between the rutile $TiO_2$ nanorods and anatase $TiO_2$ nanoparticles in our heterogeneous nanostructures. The preparation method in our study can isolate the heterogeneous nanostructures from the nonadsorbed anatase particles by repeated centrifugation and can also ensure intimate contact between the anatase particles and rutile nanorods, which has been considered to be vital for the observation of the synergistic effect.[6] Our study also shows that the strength of the synergistic effect is dependent on the number of adsorption cycles. An estimation from the rate constants shows that the samples with $n = 7$ and 9 may exhibit maximal synergistic effects.

In our photocatalytic experiment, the emission of the black-light lamp includes mainly UV light, with a peak at about 352 nm that can excite electrons into the conduction band in both anatase and rutile. Considering that very little visible light is emitted by the black-light lamp, it is reasonable to neglect any possible antenna effect of rutile in transferring energy from visible-light excitation to anatase. The charge transfer (electrons) from anatase to rutile due to the slightly lower conduction band energy of rutile[4,20] should be responsible for the improvement of the photocatalytic activity for decomposing acetaldehyde. Similar results have been reported in previous anatase/rutile heterogenerous nanostructures by simultaneously exciting the two phases.[4,6] Furthermore, such interfacial electron transfer has also been evidenced by directly observing where silver nanoparticles have been deposited (reduction sites).[4]

The photocatalytic oxidation of gaseous acetaldehyde by $TiO_2$ has been proposed[32] to involve a carbonyl-radical-mediated chain reaction, which is mediated by hydroxyl radicals, adsorbed oxygen, superoxide radicals, and/or hydrogen peroxide. These active species result from the trapping of photogenerated electrons and holes by oxygen, $H_2O$, and the hydrated surface of $TiO_2$. The charge-trapping processes can restore the photocatalyst to its original state. In addition, the oxygen in the reaction system can inhibit the formation of $Ti^{3+}$ defect sites within the bulk of $TiO_2$,[38] which also ensures the original state of the photocatalyst after the photocatalytic reaction. In our previous studies, acetic acid and formic acid were detected as the main intermediates and/or byproducts, and $CO_2$ was the final product.[39] These intermediates can be further oxidized to $CO_2$ with prolonged UV illumination,[39] which indicates that these intermediates cannot poison the photocatalyst. In the present work, we found that for the heterogenerous nanostructure with $n = 9$, after 230 min of UV irradiation almost 100% of the acetaldehyde molecules had been decomposed but only approximately 43 mol % of the acetaldehyde was mineralized to $CO_2$.

Thus, the photogenerated electrons and holes both play major roles in the oxidation of acetaldehyde. The improved photocatalytic activity of the sample with $n = 9$ with regard to decomposing acetaldehyde can be ascribed to improved charge separation resulting from an anatase porous layer with an optimized thickness. Following the charge transfer between anatase and rutile, the photogenerated electrons in the conduction of rutile can be scavenged by oxygen molecules to form superoxide radicals, which contribute to the oxidation of acetaldehyde. As shown in Figure 1c, the surface of the rutile nanorods in the sample with $n = 9$ is only partially covered by anatase nanoparticles. This allows free access of oxygen to the rutile surface. At the same time, the holes remaining in the valence band of anatase can oxidize the acetaldehyde.

However, for the sample with $n = 11$, the thickness of the anatase porous layer on the rutile nanorods becomes excessive (Figure 1d,f); the outermost anatase nanoparticles cannot form an effective interface with the rutile nanorod, so the effectiveness of charge separation is lessened. Furthermore, it becomes more difficult for the photogenerated electrons to be scavenged by oxygen because of a blocking effect (i.e., lack of free access of oxygen to the rutile surface). Finally, the resulting accumulation of the photogenerated electrons in the conduction band of rutile can increase the recombination probability with the holes in the valence band of anatase, which could also help to explain the slightly worse activity for the sample with $n = 11$, although the anatase content in this sample increases.

In summary, we have designed a heterogeneous nanostructure by depositing anatase $TiO_2$ nanoparticles on the surface of rutile $TiO_2$ nanorods using the LbL assembly technique. Synergism between anatase and rutile $TiO_2$ was observed in the decomposition of gaseous acetaldehyde, and the strength of the synergistic effect was found to be dependent on the thickness of the anatase particle layer. The present LbL assembly method shows great potential for developing highly active $TiO_2$ photocatalysts that can provide an optimization of the particle sizes of anatase and rutile, the thickness of the anatase layer, and the LbL assembly parameters. Similar methods should also be suitable for preparing heterogeneous nanostructures from other oxide semiconductors.

**Acknowledgment.** This work was supported by a Grand-in-Aid for Science Research on Priority Areas (417) from the Ministry of Education, Culture, Sports, Science and Technology (MEXT) of the Japanese Government and by the Core Research for Evolutional Science and Technology (CREST) Program of the Japan Science and Technology (JST) Agency. Z.L. acknowledges the Japan Society for the Promotion of Science (JSPS) for a Postdoctoral Fellowship for Foreign Researchers.

**Supporting Information Available:** Detailed procedures to establish a standard calibration curve for the measurement of the weight fractions of anatase and rutile $TiO_2$ in the heterogeneous nanostructures. Normalized diffuse UV−visible absorption spectra of rutile $TiO_2$ nanorods and the heterogeneous nanostructure with $n = 11$. This information is available free of charge via the Internet at http://pubs.acs.org.

LA7018023

(38) Howe, R. F.; Grätzel, M. *J. Phys. Chem.* **1987**, *91*, 3906−3909.
(39) Noguchi, T.; Fujishima, A.; Sawunyama, P.; Hashimoto, K. *Environ. Sci. Technol.* **1998**, *32*, 3831−3833.